Acta Crystallographica Section B
Structural Science
ISSN 0108-7681

Mechanism of the morphotropic transformation between the rutile and corundum structural types

H. Katzke[a]* and R. Schlögl[b]

[a]Universität Kiel, Institut für Geowissenschaften, Kristallographie, Olshausenstrasse 40, 24098 Kiel, Germany, and [b]Fritz-Haber-Institut der Max-Planck-Gesellschaft, Abteilung Anorganische Chemie, Faradayweg 4–6, 14195 Berlin, Germany

Correspondence e-mail: hanne@min.uni-kiel.de

Received 3 March 2003
Accepted 16 May 2003

The rutile/corundum structural transformation which is based on crystallographic shear is discussed in terms of a one-dimensional disorder model. The transformation process is described by a simple model based on the structural relationship between the rutile-type and corundum-type phases. The model is able to handle randomly spaced crystallographic shear planes, the so-called Wadsley defects, as well as clustered CS planes. Calculations hsow that simply modifying the probability parameters of the model can lead to phase segregation. X-ray powder diffraction patterns are calculated for the proposed transformation mechanism as a function of the stoichiometry x in MO_{2-x} in order to show the influence of such defects on the intensities and linewidths of the Bragg reflections.

1. Introduction

Morphotropic transformations can be defined as the transitions occurring between phases which differ in their composition (Tolédano *et al.*, 2001). They are found in open systems such as solid solutions or complex fluid systems and constitute one of the most essential problems posed by the formation of minerals. At present no theoretical framework exists which allows a description of morphotropic transformations because the basic ingredients needed for this description, *i.e.* the transformation mechanisms, are not yet well understood. The aim of the present work is to describe theoretically a possible transformation mechanism between the rutile and corundum structural types, which are among the most common structures found in minerals. They correspond, respectively, to the stoichiometries MO_2 and M_2O_3, where M is a transition metal, and are obtained, for example, during the reduction of the oxides TiO_2, VO_2, CrO_2 *etc.* In the Ti—O and V—O system additional phases forming a homologous series between MO_2 and M_2O_3 are known, the so-called Magnéli phases of the general formula M_nO_{2n-1} (Hyde & Andersson, 1989). The crystallographic shear operation transforming MO_2 into M_nO_{2n-1} (Katzke & Schlögl, 2003) cannot explain the formation of the corundum-type structure. Therefore, in the present paper another crystallographic shear mechanism is proposed enabling a direct transformation of the rutile-type into the corundum-type structure. Hyde & Bursill (1969) mentioned the importance of disordered states during the transformation from one structure to another. We will demonstrate that the MO_2–M_2O_3 transformation can be described in terms of a one-dimensional disorder model, in which the crystallographic shear planes are regarded as chemical defects.

Crystallographic shear planes can be interpreted as chemical defects, as long as they are not a fundamental part of

the structure and do not interact with each other. However, at sufficiently high defect concentrations a model with non-interacting, randomly spaced crystallographic shear planes is not plausible. The stress around Wadsley defects should force them to order, and a clustering of defects and thus a microdomain texture may result from this ordering effect. The microdomain model assumes that two related and ordered structures coexist in the crystal, dispersed aperiodically but coherently one into the other. Both phenomena, randomly spaced, shear planes and microdomains of different phases, have been observed by X-ray and electron diffraction experiments in non-stoichiometric phases (Hyde & Bursill, 1969). This problem is considered here theoretically for the example of the rutile/corundum transformation.

2. Structural relationship between the rutile and the corundum structure

The aim of the present paper is to treat the rutile/corundum transformation as generally as possible. However, whenever lattice parameters and atomic coordinates for structural comparisons, and scattering factors for X-ray intensity calculations are needed, the system VO_2/V_2O_3 is selected.

VO_2 crystallizes in the rutile structure. The tetragonal unit cell has lattice parameters $a = 4.555$ and $c = 2.851$ Å. The space group is $P4_2/mnm$ (McWhan *et al.*, 1974). Two V atoms occupy the Wyckoff position 2(*a*):(0 0 0) and four O atoms occupy the Wyckoff position 4(*f*): (0.3001 0.3001 0). The structure may be described as a distorted hexagonal close-packed array of O atoms with the V^{4+} cations occupying half of the octahedral sites. The VO_6 octahedra share edges in the **c** direction and corners along [110] and [$\bar{1}$10].

V_2O_3 crystallizes in the corundum structure. The hexagonal unit cell has lattice parameters $a = 4.949$ and $c = 13.998$ Å. The space group is $R\bar{3}c$ (Rice & Robinson, 1977). There are 12 V atoms which occupy the Wyckoff position 12(*c*): (0 0 0.34634) and 18 O atoms occupy the Wyckoff position 18(*e*): (0.3122 0 1/4). The structure may be described as an approximately hexagonal close-packed array of oxide ions with the V^{3+} cations in two-thirds of the octahedral sites. The cation arrangement leads to a tripling of the **c** axis relative to the hexagonal ...*AB*... stacking sequence. The structure is built up of pairs of VO_6 octahedra sharing faces along **c**. Such pairs form chains by edge-sharing in the plane perpendicular to **c**. These chains are linked to other equivalent chains by edge-sharing, thus forming a three-dimensional network.

In order to point out the structural relationships between the rutile and corundum types, the structures of VO_2 and V_2O_3 are transformed into a common orientation. The crystallographic transformations performed are summarized in

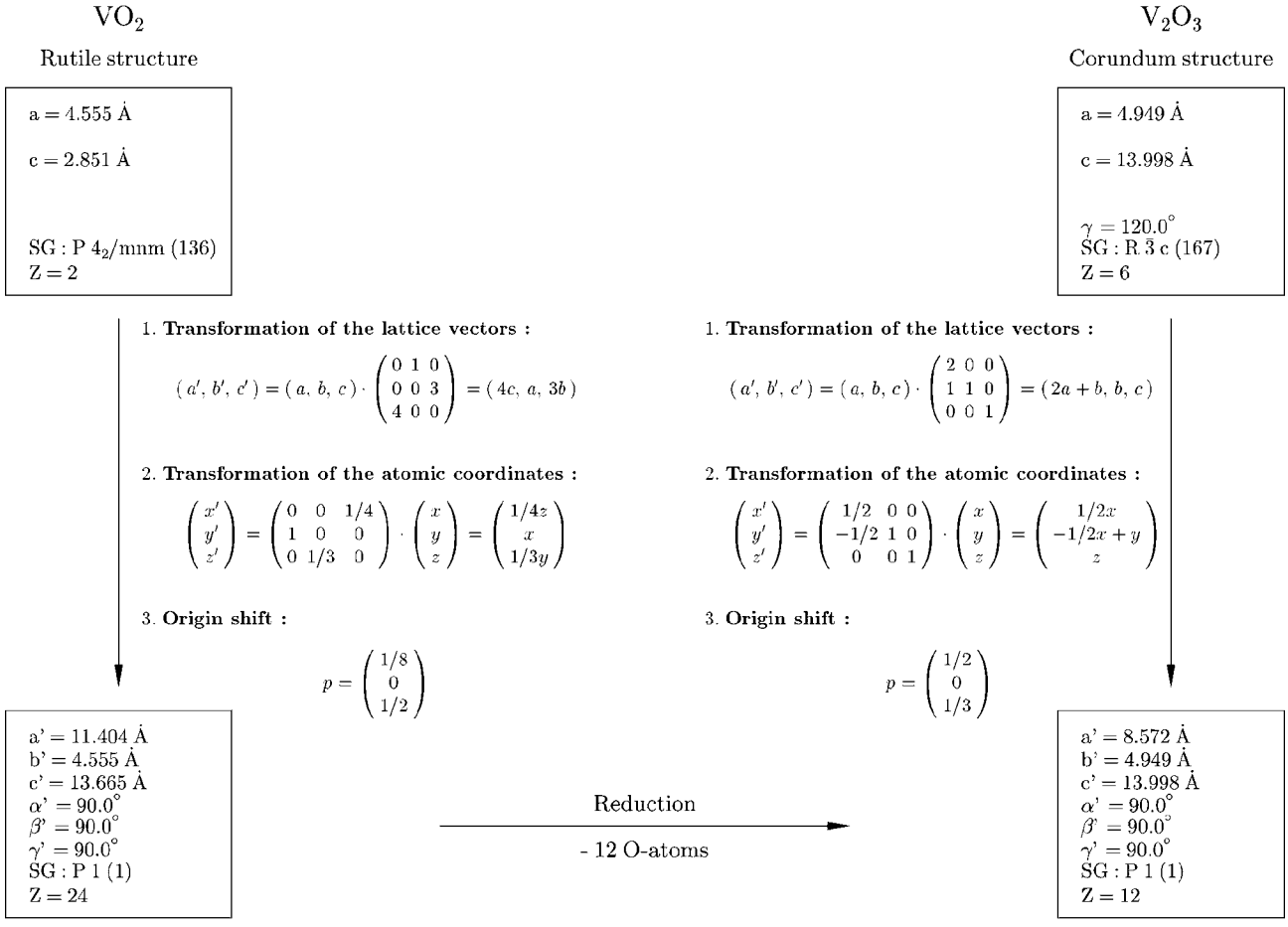

Figure 1
Diagram of the necessary transformations in order to compare the structures of VO_2 and V_2O_3.

Fig. 1. The tetragonal rutile unit cell of VO_2 is transformed into an orthorhombic supercell which is 12 times larger with basis vectors $\mathbf{a}' = 4\mathbf{c}$, $\mathbf{b}' = \mathbf{a}$ and $\mathbf{c}' = 3\mathbf{b}$. The new lattice parameters are $a' = 11.404$, $b' = 4.555$ and $c' = 13.665$ Å. In order to enable a direct comparison of all the atomic positions, the symmetry $P1$ is used. The atomic coordinates for the supercell are related to the rutile cell by the following relations: $x' = 1/4\ z$, $y' = x$ and $z' = 1/3\ y$. An origin shift of $p = (1/8\ 0\ 1/2)$ is introduced such that the origins of the rutile and corundum structure coincide.

The hexagonal unit cell of V_2O_3 is transformed into a C-centred orthohexagonal cell, as explained in the *International Tables for Crystallography* (1989, Vol. A), with lattice vectors $\mathbf{a}' = 2\mathbf{a} + \mathbf{b}$, $\mathbf{b}' = \mathbf{b}$ and $\mathbf{c}' = \mathbf{c}$. The new lattice parameters are $a' = 8.572$, $b' = 4.949$ and $c' = 13.998$ Å. The atomic coordinates for the orthohexagonal cell are related to the hexagonal cell by the relations $x' = 1/2x$, $y' = -1/2x + y$ and $z' = z$. The new basis vectors are fixed at the new origin by applying an origin shift of $p = (1/2\ 0\ 1/3)$. As explained for the transformation of the rutile structure, the hexagonal structure of V_2O_3 is transformed into a cell with an orthorhombic metric, but described in space group $P1$. The transformed unit cells of VO_2 and V_2O_3 are shown in Fig. 2. The cells contain 24 V atoms; the orthorhombic rutile cell contains 48 O atoms and the orthohexagonal unit cell of V_2O_3 contains 36 O atoms. The reduction from VO_2 to V_2O_3 nominally requires the removal of 12 O atoms per unit cell. These are shown as white circles in the left half of Fig. 2. The O atoms are regularly arranged on certain planes. These planes interrupt the rutile structure in a periodic manner. For a better understanding of the structural changes, the regions between the oxygen planes are painted in light and dark grey. These regions of preserved rutile structure are termed rutile slabs. In the structure of VO_2 neighbouring rutile slabs are topologically equivalent. The removal of the marked O atoms causes the condensation of the rutile structure which is associated with a displacement of the neighbouring rutile slabs by $[+1/8\ -1/2\ 0]$ relative to the supercell of VO_2. In the corundum structure, neighbouring rutile slabs, painted in light and dark grey, are therefore displaced by $1/2\mathbf{b}'$.

The rutile/corundum transformation can be described by crystallographic shear (Hyde & Andersson, 1989). The planes, where the O atoms are removed, are called the crystallographic shear (CS) planes (Wadsley, 1955). The CS planes are the sites where the oxygen-deficiency is compensated for by condensing the structure. The crystallographic shear planes are parallel to (400) of the orthorhombic rutile supercell. The shear operation (400) $[1/8\ -1/2\ 0]$ can be transformed back into the original unit cell of the rutile structure by the following transformations:

$$(h\,k\,l) = (4\,0\,0) \cdot \begin{pmatrix} 0 & 0 & 1/4 \\ 1 & 0 & 0 \\ 0 & 1/3 & 0 \end{pmatrix} = (0\,0\,1); \qquad (1)$$

$$\begin{bmatrix} u \\ v \\ w \end{bmatrix} = \begin{pmatrix} 0 & 1 & 0 \\ 0 & 0 & 3 \\ 4 & 0 & 0 \end{pmatrix} \cdot \begin{bmatrix} +1/8 \\ -1/2 \\ 0 \end{bmatrix} = \begin{bmatrix} -1/2 \\ 0 \\ +1/2 \end{bmatrix}. \qquad (2)$$

After transformation the CS operator is (001) 1/2 $[\bar{1}01]$ based on the tetragonal rutile cell. Between the crystallographic shear planes, normal regions of the rutile structure are preserved. The atomic displacements, associated with the transformation within one individual rutile slab, are small and range from 0.07 to 0.18 Å for V atoms and from 0.16 to 0.39 Å for O atoms.

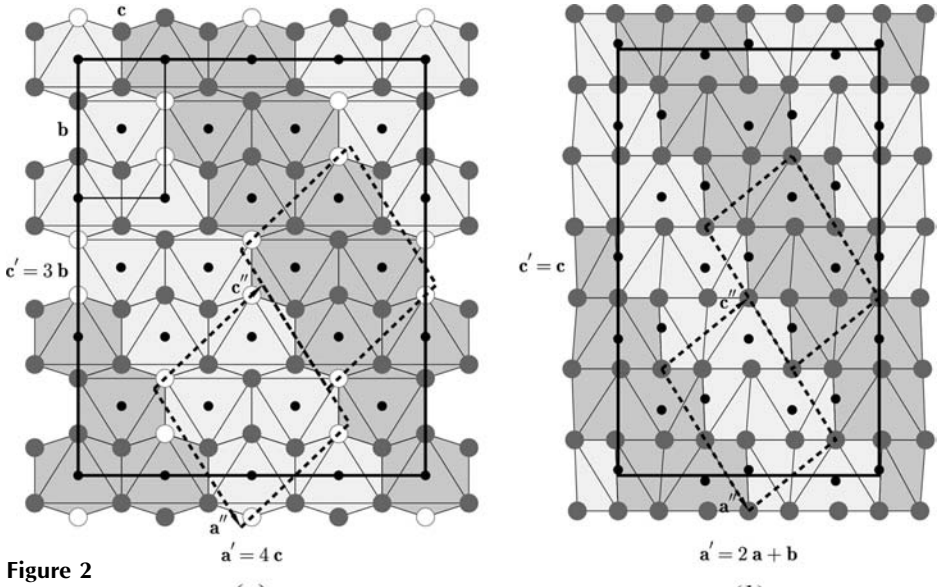

Figure 2
The structures of (*a*) rutile-type VO_2 and (*b*) corundum-type V_2O_3, projected along $\mathbf{b}'$. The transformed unit cells are indicated by solid lines. In (*a*) the original tetragonal unit cell of the rutile structure is also shown by solid lines. V atoms are represented by small black circles and O atoms by large grey circles. O atoms which will be removed by the proposed reduction mechanism are shown by large white circles. Neighbouring 'rutile slabs', as defined in the text, are painted in light and dark grey. In the rutile structure neighbouring 'rutile slabs' are at the same height; in the corundum structure light and dark grey 'corundum slabs' are displaced by $1/2\mathbf{b}'$. The smallest building units within the respective structures, which were used in the calculations, are shown by broken lines in (*a*) and (*b*). The stacking of the units along $\mathbf{c}''$ is indicated. The transformations to obtain $\mathbf{a}''$, $\mathbf{b}''$ and $\mathbf{c}''$ are explained in the text.

3. Model calculations for randomly spaced CS planes

For the rutile/corundum transition the following model can be proposed. The first step in the schematic reduction process involves the formation of vacant oxygen sites together with the reduction of V^{4+} to V^{3+}. The vacant oxygen sites are not distributed at random but are located on (001) planes of the tetragonal rutile cell. To avoid having whole layers of vacant sites, condensation of the structure occurs by crystallographic shear, $(001)1/2[\bar{1}01]$, eliminating the vacan-

cies and forming CS planes. As a result of condensation, the octahedra within the CS planes share faces, whereas in unreduced regions of rutile the octahedra remain linked by edge-sharing. In the corundum structure, the CS planes form an ordered arrangement, therefore, they are a fundamental part of the structure and should not be regarded as defects. However, during the reduction of VO_2 to V_2O_3, the variation in stoichiometry can be accommodated by increasing the number of CS planes and decreasing the number of rutile slabs between adjacent CS planes. The randomly spaced CS planes form extended two-dimensional defects, which are known as Wadsley defects (Wadsley, 1955).

For the above model, we have calculated the X-ray diffraction intensities as a function of the stoichiometry parameter x in VO_{2-x}. The rutile slabs in the structures of VO_2 and V_2O_3 are stacked along [011] relative to the tetragonal cell of rutile. The smallest structural units necessary to build up the structures of VO_2 and V_2O_3 are shown by broken lines in Fig. 2. The axes of the rutile unit are obtained by the transformation $\mathbf{a}'' = \mathbf{b} + \mathbf{c}$, $\mathbf{b}'' = \mathbf{a}$ and $\mathbf{c}'' = -3/4\mathbf{b} + 5/4\mathbf{c}$. They are $a'' = 5.374$, $b'' = 4.555$, $c'' = 4.937$ Å and $\beta'' = 101.75^\circ$. The atomic coordinates transform according to $x'' = 5/8y + 3/8z$, $y'' = x$ and $z'' = -1/2y + 1/2z$. An origin shift of $p = (0.56256\ 0\ 1/4)$ is introduced to bring the origin of the rutile unit into the proper position.

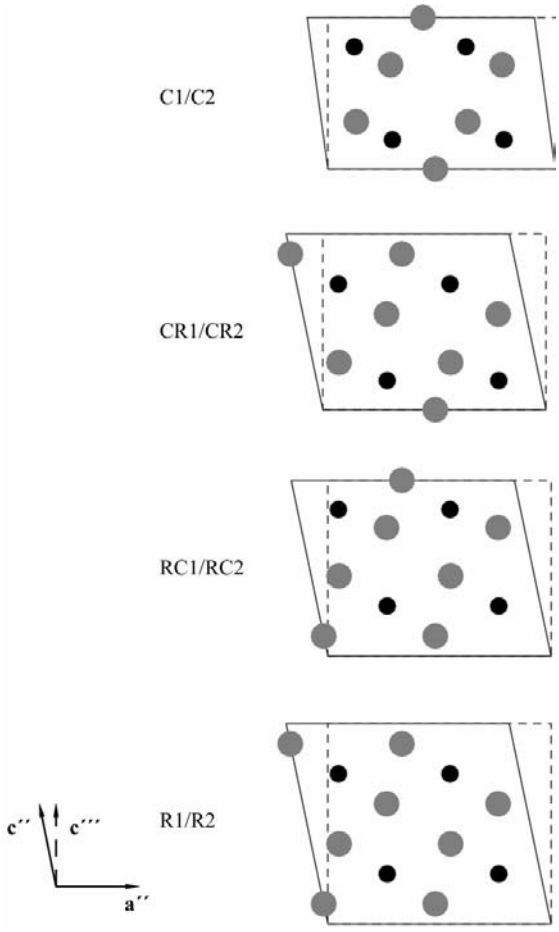

Figure 3
Structures of the building units R1/R2, RC1/RC2, CR1/CR2 and C1/C2 projected along $\mathbf{b}''$. V atoms are represented by smaller black circles and O atoms by larger grey circles.

Table 1
Probability matrix used for calculating X-ray powder diffraction intensities for randomly spaced CS planes.

	R1	R2	RC1	RC2	CR1	CR2	C1	C2
R1	P	0.0	$1-P$	0.0	0.0	0.0	0.0	0.0
R2	0.0	P	0.0	$1-P$	0.0	0.0	0.0	0.0
RC1	0.0	0.0	0.0	0.0	0.0	P	0.0	$1-P$
RC2	0.0	0.0	0.0	0.0	P	0.0	$1-P$	0.0
CR1	P	0.0	$1-P$	0.0	0.0	0.0	0.0	0.0
CR2	0.0	P	0.0	$1-P$	0.0	0.0	0.0	0.0
C1	0.0	0.0	0.0	0.0	0.0	P	0.0	$1-P$
C2	0.0	0.0	0.0	0.0	P	0.0	$1-P$	0.0

The axes of the corundum unit are obtained by the transformation $\mathbf{a}'' = 1/3\mathbf{a}' - 1/3\mathbf{c}'$, $\mathbf{b}'' = \mathbf{b}'$ and $\mathbf{c}'' = 1/3\mathbf{a}' + 1/6\mathbf{c}'$ related to the corundum supercell shown in Fig. 2. The axes of the corundum unit are $a'' = 5.471$, $b'' = 4.949$, $c'' = 3.689$ Å and $\beta'' = 97.75^\circ$. The atomic coordinates are obtained by the transformation $x'' = x' - 2z'$, $y'' = y'$ and $z'' = 2x' + 2z'$. An origin shift of $p = (1/6\ 0\ 1/4)$ is introduced in order to match the origin of the corundum unit onto that of the defined rutile unit.

In the rutile structure adjacent rutile units are displaced by $-1/4\mathbf{a}''$. In the corundum structure neighbouring corundum units are displaced by $1/2(\mathbf{a}'' + \mathbf{b}'')$. Altogether, the simulation of a disordered structure VO_{2-x} in direct space requires the definition of eight different structural units: two for the rutile structure (R1/R2), two for the corundum structure (C1/C2), two mixed rutile/corundum (RC1/RC2) and two corundum/rutile units (CR1/CR2) describing the transition from the rutile to the corundum and from the corundum to the rutile structure. The mixed rutile/corundum and corundum/rutile units are necessary in order to guarantee that the nearest-neighbour relationships are preserved at the Wadsley defect. The basic structural units are shown in Fig. 3 projected along $\mathbf{b}''$. Atomic coordinates for the units R2, RC2, CR2 and C2 are obtained from the atomic coordinates of the units R1, RC1, CR1 and C1 by the transformation $x_2'' = x_1''$, $y_2'' = y_1'' + 1/2$ and $z_2'' = z_1''$. Randomly spaced CS planes are modelled by the probabilities given in Table 1. The parameter P defines the probability of finding a rutile slab as the next slab. Therefore, the probability $1 - P$ defines the Wadsley defect probability of finding a single crystallographic shear plane within a rutile matrix. All probability parameters which are zero in Table 1 characterize the forbidden slab sequences; their values are always zero.

The average intensity distribution for disordered VO_{2-x} was calculated as described by Katzke (2002). The calculations were performed with the powder version *PSIM* of the program *fv*1 written by Kato (Kato *et al.*, 1990). The program applies the matrix method of Kakinoki & Komura (1965). The resolution function was assumed to be a Lorentzian with

variable *uvw* parameters given as a function of 2θ according to (3) (Cagliotti *et al.*, 1958), so

$$FWHM^2 = u\tan^2\theta + v\tan\theta + w. \quad (3)$$

The *uvw* parameters $u = 0.1116$, $v = -0.0893$ and $w = 0.0588$ were used to describe typical reflection profiles for a standard powder X-ray diffraction experiment. Atomic scattering factors for neutral atoms and their dispersions are taken from the *International Tables for Crystallography* (1992, Vol. C).

Owing to the different monoclinic angles of the structural units, the calculations were performed in an orthogonal system with $a''' = a''$, $b''' = b''$ and $c''' = c''\sin\beta''$. The increase in the a'''- and b'''-lattice parameters associated with the transformation from VO_2 to V_2O_3 is taken into account by a linear change from $a''' = 5.374$ Å for VO_2 to $a''' = 5.471$ Å for V_2O_3 and $b''' = 4.555$ Å for VO_2 to $b''' = 4.949$ Å for V_2O_3 as a function of the probability *P*. c''' has a value of 4.8336 Å. The monoclinic angles and the displacements along $\mathbf{a}'''$ are expressed by the *x* component of the stacking vector. The different slab thicknesses are considered by the *z* component of the stacking vector.

The calculated X-ray diffraction patterns for VO_2, V_2O_3 and oxygen-deficient VO_{2-x} are shown in Fig. 4. The X-ray diffraction pattern of VO_2 is calculated with a probability $P = 1$, that for V_2O_3 with $P = 0$. The X-ray diffraction patterns for oxygen-deficient VO_{2-x} are obtained for $0.0 < P < 1.0$. The average valence of the vanadium ions can be calculated from the probability elements of Table 1 according to

$$V_{\rm av} = P\,V_{\rm VO_2} + (1-P)\,V_{\rm V_2O_3}, \quad (4)$$

where $V_{\rm av}$ is the average valence of V in the disordered phases, $V_{\rm VO_2}$ and $V_{\rm V_2O_3}$ are the valence of V in VO_2 and V_2O_3. *P* and $(1-P)$ are the probabilities as defined in Table 1.

With increasing Wadsley defect density, the correlation length of the rutile domains decreases, whereas the correlation length of corundum domains simultaneously increases. The domain structure influences the intensities and linewidths of all the reflections, however some reflection classes are particularly strongly influenced by the disorder. These reflections are *hk*0 reflections with $h = 2n + 1$ of rutile VO_2. Their widths increase continuously with increasing stacking fault probability; finally these reflections vanish in the background. See, for example, the variation of the reflection profiles and intensities of the reflections 110_r at $2\theta = 27.67^\circ$ and 310_r at $2\theta = 64.66^\circ$. Indices are related to the original tetragonal unit cell of rutile VO_2. Wadsley defects in the structure of V_2O_3 strongly influence reflections of the classes *hkl*, *h*0*l* and 0*kl*, the classes *hk*0, 00*l* and *hhl* are less affected. This can be seen by comparing the variations in reflection profiles and intensities for the reflections 012_c at $2\theta = 24.33^\circ$, 104_c at $2\theta = 33.02^\circ$, 300_c at $2\theta = 65.26^\circ$ and 110_c at $2\theta = 36.28^\circ$. The indices are related to the original hexagonal unit cell of the corundum-type structure V_2O_3. Fig. 4 reveals that the symmetry change from tetragonal $P4_2/mnm$ to hexagonal $R\bar{3}c$, which is associated with the rutile/corundum transformation, results directly from the disorder model. As mentioned above, no symmetry constraints were used; all calculations were performed in space group *P*1. Peaks shift because of the increase in the a''' and b''' lattice parameters associated with the transition from VO_2 to V_2O_3.

Fig. 5 shows the volume fractions of rutile and corundum slabs together with the fraction of Wadsley defects as a func-

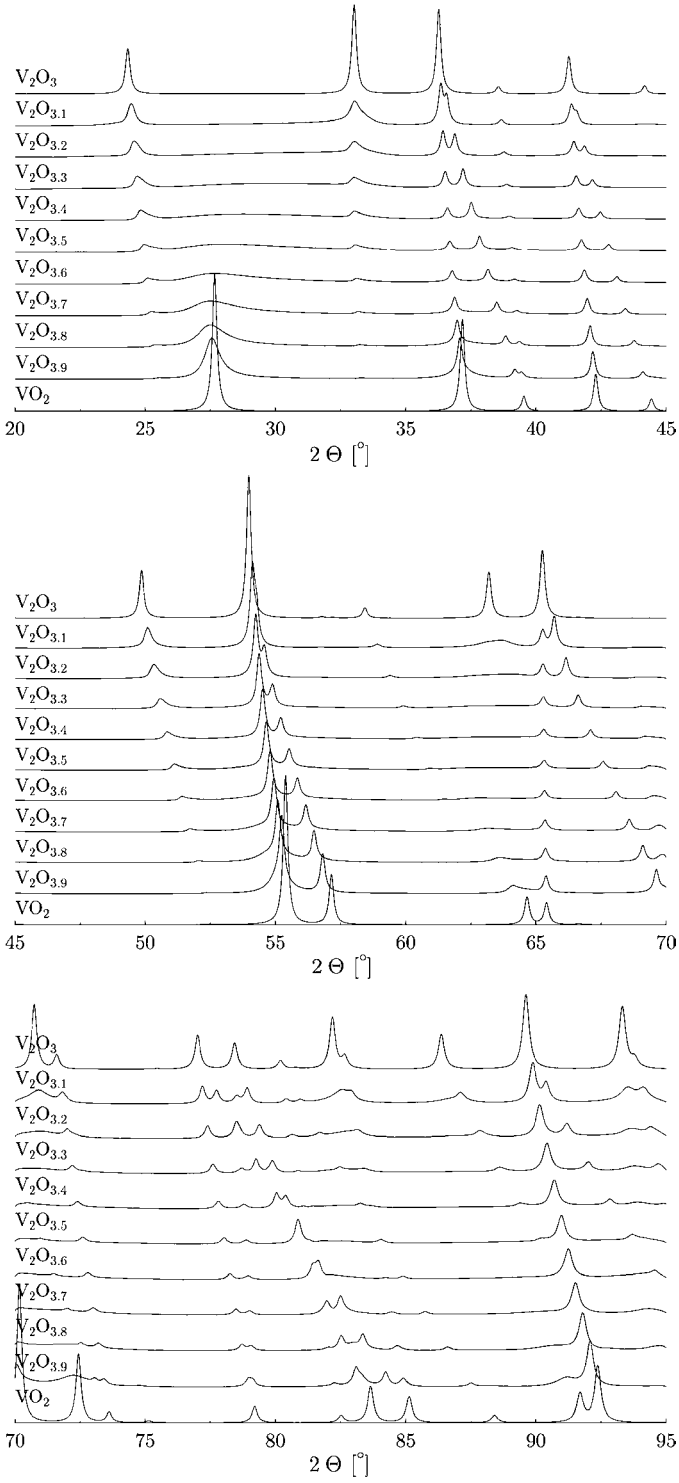

Figure 4
Calculated X-ray diffraction patterns for the chemical transformation of rutile-type VO_2 to corundum-type V_2O_3, assuming a model with randomly spaced CS planes for reduced phases VO_{2-x} ($\lambda = 1.54056$ Å).

Table 2
Probability matrix used for calculating X-ray powder diffraction intensities for clustered CS planes.

	R1	R2	RC1	RC2	CR1	CR2	C1	C2
R1	P_1	0.0	$1-P_1$	0.0	0.0	0.0	0.0	0.0
R2	0.0	P_1	0.0	$1-P_1$	0.0	0.0	0.0	0.0
RC1	0.0	0.0	0.0	0.0	0.0	$1-P_2$	0.0	P_2
RC2	0.0	0.0	0.0	0.0	$1-P_2$	0.0	P_2	0.0
CR1	P_1	0.0	$1-P_1$	0.0	0.0	0.0	0.0	0.0
CR2	0.0	P_1	0.0	$1-P_1$	0.0	0.0	0.0	0.0
C1	0.0	0.0	0.0	0.0	0.0	$1-P_2$	0.0	P_2
C2	0.0	0.0	0.0	0.0	$1-P_2$	0.0	P_2	0.0

tion of the average valence of V. Starting from VO_2 the oxygen deficiency is accommodated by an increasing number of Wadsley defects and a decreasing number of rutile slabs between adjacent Wadsley defects. For a non-stoichiometric compound of nominal composition $V_2O_{3.5}$, the number of Wadsley defects is a maximum with a value of 50%. Further reduction will successively decrease the number of Wadsley defects and increase the number of ordered crystallographic shear planes. In the structure of V_2O_3 no Wadsley defects are present and the structure is again long-range ordered. Consequently, for V_2O_3 the reflections are as sharp as those of VO_2.

Experimental support for the proposed model can be obtained from electron diffraction patterns of reduced rutile. These patterns show an intense streaking along **g** = 101 owing to the high density of {101} faults (see, for example, Fig. 22 in Hyde & Bursill, 1969). Nevertheless, the proposed model considers one extreme case: the total absence of interactions between single crystallographic shear planes leading to randomly spaced CS planes. The fraction of such Wadsley defects is certainly dependent on the history of crystal treatment, in particular, on the temperature. However, also at very high temperatures it is still hard to believe that the end members (or rather 'structural motives') could coexist locally in equilibrium at any temperature. Presumably, randomly spaced defects should dominate at very high temperatures and for slightly reduced phases near the end members VO_2 and V_2O_3. For higher degrees of reduction and at low tempera-

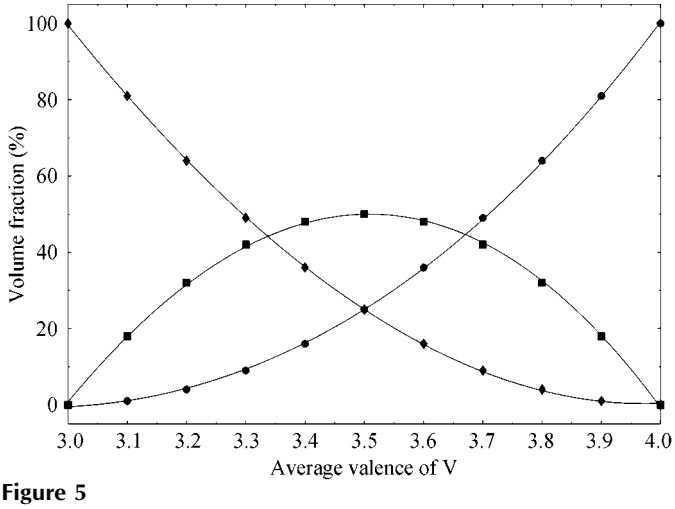

Figure 5
Volume fractions of the different structural units as a function of the average valence of the V atoms: filled circles: rutile slabs; filled diamonds: corundum slabs; filled squares: Wadsley defects.

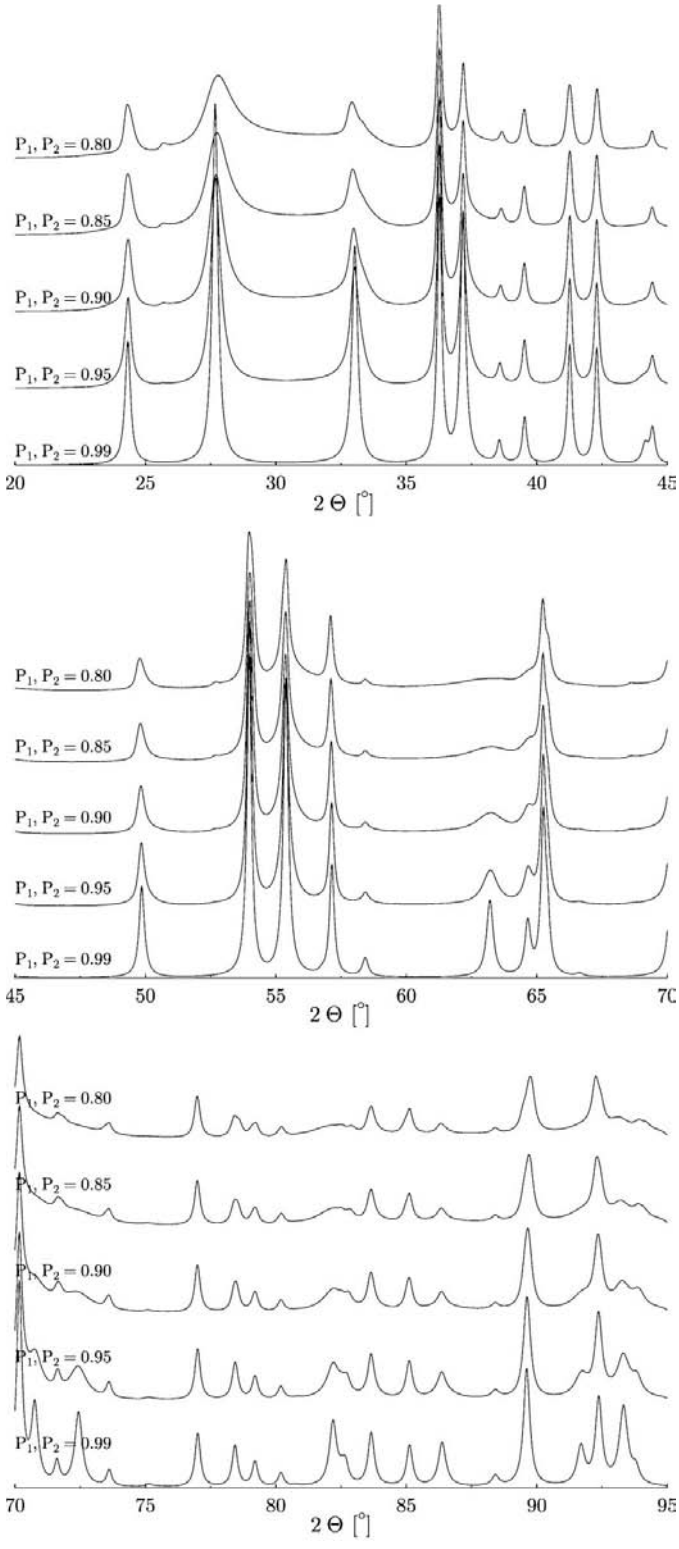

Figure 6
Calculated X-ray diffraction patterns for clustered CS planes leading to a phase separation VO_2/V_2O_3. The volume fractions of the two phases are 50% each ($P_1 = P_2$). The degree of disorder within the two phases increases with decreasing P (λ = 1.54056 Å).

tures, phase separation should occur due to a clustering of defects.

4. Model calculations for clustered CS planes

Such a clustering of CS planes can be simulated with the former disorder model by introducing another probability parameter P_2. The probability matrix is given in Table 2. Herein, the parameter P_1 defines the probability of finding a rutile slab as the next slab, the parameter P_2 defines the probability of finding a corundum slab as the next slab, the parameter $1 - P_1$ defines the probability of finding Wadsley defects within a rutile matrix and the parameter $1 - P_2$ defines the probability of finding Wadsley defects within a corundum matrix. Again, all matrix elements P_{ij} which are zero characterize forbidden slab sequences. A clustering of CS planes is expressed by high probabilities P_1 and P_2. This case corresponds to the observation of Ubbelohde (1966), that when the structures are closely related the transformation proceeds *via* a 'hybrid' crystal, in which domains of both phases coexist.

Calculated X-ray powder diffraction patterns are shown in Fig. 6. The ordering state of the two phases and their volume fractions are defined by the values of P_1 and P_2. For well ordered phases (P_1 and P_2 are close to one), the diffraction pattern is similar to that obtained from a mixture of both phases. CS planes, interrupting the regular sequence of rutile slabs on one hand and corundum slabs on the other hand, have the same influence on the intensities and linewidths of reflections as discussed for randomly spaced CS planes, unless the two phases are observed simultaneously. Therefore, clustered CS planes leading to a phase separation are not considered here in greater detail.

5. Conclusions

The rutile/corundum transformation which is based on the crystallographic shear of two closely related structures is discussed in terms of a simple disorder model. The model is able to handle randomly spaced and clustered CS planes. The clustering of CS planes leads to the formation of hybrid crystals, in which domains of both phases coexist. In real systems, the transition might be continuous. Presumably, randomly spaced CS planes should dominate at high temperatures and for slightly reduced phases near the end members (the rutile-type and corundum-type structures). For higher defect concentrations the local strain around Wadsley defects, arising from the substantial ($\sim$10%) difference in the axes of the rutile and corundum structural units, should force the defects to order, so that a phase separation should be observed. X-ray intensity calculations have been performed for both, randomly spaced and clustered CS planes, in order to show the influence of such defects on intensities and linewidths of reflections. With the proposed model a continuous transition from randomly spaced to ordered crystallographic shear planes can be described by simply modifying the probability parameters of the model. From this point of view, the model should be to some extent universal. As far as experimental data have been available from the literature (Hyde & Bursill, 1969), the model is in accordance with them. However, to our knowledge *in situ* X-ray diffraction studies have not yet been performed on these systems, therefore, a small uncertainty about the transferability of the model to real chemical transformations remains. Nevertheless, the theoretical study confirms the possibility of studying the distribution of Wadsley defects by X-ray diffraction. Keeping in mind that such defects are normally studied by electron microscopy, but that this method is a locally probing method, X-ray powder diffraction seems to be a powerful complementary technique for studying and quantifying these kinds of defects.

The work is supported by SFB 546 of the Deutsche Forschungsgemeinschaft (DFG). One of the authors (HK) would like to thank P. Tolédano and M. Czank for valuable discussions.

References

Cagliotti, G., Paoletti, A. & Ricci, F. P. (1958). *Nucl. Instrum.* **3**, 223–228.
Hyde, B. G. & Andersson, S. (1989). *Inorganic Crystal Structures*. New York: Wiley.
Hyde, B. G. & Bursill, L. A. (1969). *The Chemistry of Extended Defects in Non-metallic Solids*, edited by L. Eyring and M. O'Keeffe, pp. 347–378. Amsterdam: North-Holland.
Kakinoki, J. & Komura, Y. (1965). *Acta Cryst.* **19**, 137–147.
Kato, K., Kosuda, K., Koga, T. & Nagasawa, H. (1990). *Acta Cryst.* C**46**, 1587–1590.
Katzke, H. (2002). *Z. Kristallogr.* **217**, 127–130.
Katzke, H. & Schlögl, R. (2003). *Z. Kristallogr.* **218**, 432–439..
McWhan, D. B., Marezio, M., Remeika, J. P. & Dernier, P. D. (1974). *Phys. Rev. B*, **10**, 490–495.
Rice, C. E. & Robinson, W. R. (1977). *J. Solid State Chem.* **21**, 145–154.
Tolédano, J.-C., Berry, R. S., Brown, P. J., Glazer, A. M., Metselaar, R., Pandey, D., Perez-Mato, J. M., Roth, R. S. & Abrahams, S. C. (2001). *Acta Cryst.* A**57**, 614–626.
Ubbelohde, A. R. (1966). *J. Chim. Phys.* **62**, 33–42.
Wadsley, A. D. (1955). *Rev. Pure Appl. Chem.* **5**, 165–193.